ACS APPLIED MATERIALS & INTERFACES

Research Article

www.acsami.org

# Enhancement of Osteogenesis and Biodegradation Control by Brushite Coating on Mg−Nd−Zn−Zr Alloy for Mandibular Bone Repair

Xingmin Guan,[†,⊥] Meiping Xiong,[‡,⊥] Feiyue Zeng,[‡] Bin Xu,[‡] Lingdi Yang,[‡] Han Guo,[§] Jialin Niu,[†] Jian Zhang,[†] Chenxin Chen,[†] Jia Pei,[†] Hua Huang,[†] and Guangyin Yuan*[,†]

[†]National Engineering Research Center of Light Alloys Net Forming and State Key Laboratory of Metal Matrix Composite, Shanghai Jiao Tong University, Shanghai 200240, People's Republic of China

[‡]Department of Stomatology, The Fifth People's Hospital of Shanghai, Fudan University, Shanghai 200240, People's Republic of China

[§]Shanghai Synchrotron Radiation Facility, Shanghai Institute of Applied Physics, Chinese Academy of Sciences, Shanghai 201204, People's Republic of China

**ABSTRACT:** To diminish incongruity between bone regeneration and biodegradation of implant magnesium alloy applied for mandibular bone repair, a brushite coating was deposited on a matrix of a Mg−Nd−Zn−Zr (hereafter, denoted as JDBM) alloy to control the degradation rate of the implant and enhance osteogenesis of the mandible bone. Both in vitro and in vivo evaluations were carried out in the present work. Viability and adhesion assays of rabbit bone marrow mesenchyal stem cells (rBM-MSCs) were applied to determine the biocompatibility of a brushite-coated JDBM alloy. Osteogenic gene expression was characterized by quantitative real-time polymerase chain reaction (RT-PCR). Brushite-coated JDBM screws were implanted into mandible bones of rabbits for 1, 4, and 7 months, respectively, using 316L stainless steel screws as a control group. In vivo biodegradation rate was determined by synchrotron radiation X-ray microtomography, and osteogenesis was observed and evaluated using Van Gieson's picric acid-fuchsin. Both the naked JDBM and brushite-coated JDBM samples revealed adequate biosafety and biocompatibility as bone repair substitutes. In vitro results showed that brushite-coated JDBM considerably induced osteogenic differentiation of rBM-MSCs. And in vivo experiments indicated that brushite-coated JDBM screws presented advantages in osteoconductivity and osteogenesis of mandible bone of rabbits. Degradation rate was suppressed at a lower level at the initial stage of implantation when new bone tissue formed. Brushite, which can enhance oeteogenesis and partly control the degradation rate of an implant, is an appropriate coating for JDBM alloys used for mandibular repair. The Mg−Nd−Zn−Zr alloy with brushite coating possesses great potential for clinical applications for mandibular repair.


**KEYWORDS:** *Mg−Nd−Zn−Zr alloy, brushite coating, mandibular repair, degradation control, synchrotron radiation*

## 1. INTRODUCTION

Magnesium alloys, due to their biodegradability and similar Young's modulus to that of human bone, have emerged as a new class of implant biomaterials used in orthopedic applications.[1−4] Previous research only includes the study of performance of magnesium alloys in long bones such as guinea pig femurs, rat femurs, rabbit femurs and tibias, and sheep hip bones.[5−10] However, flat bones develop differently from long bones, resulting in different organic and inorganic phases.[11] Flat bones such as mandibles endure discrepant loadings compared to long bones such as tibias. Moreover, blood flow is another variation because it differs depending on the region of the body. Consequently, performance of degradable magnesium alloys applied to flat-bone repair should be investigated ulteriorly. In the present work, we implanted biodegradable Mg alloy screws made of a patented biomagnesium alloy (hereafter, denoted as JDBM)[12] and 316L stainless steel screws as control groups in mandibles of New Zealand white rabbits to determine the characteristics of degradation, biocompatibility, and osteogenesis.

Nevertheless, the incongruity between degradation rate of implant and bone regeneration appears to be a major obstruction for further applications of Mg and Mg alloys.[5,13] In the present work, a patented novel magnesium alloy, Mg-3.1Nd-0.2Zn-0.4Zr, is adopted for its uniquely uniform degradation mechanism. It has been proven to exhibit proper mechanical properties, adequate biocompatibility, and favorable degradability[14−16] for bone repair. Additionally, to further enhance biocorrosion resistance and to obtain a more bioactive layer between JDBM alloy and mandible bone, a brushite coating was

**Received:** September 23, 2014
**Accepted:** October 24, 2014
**Published:** October 24, 2014

**Table 1. Sequences of RT-PCR Primers**

| gene | primer sequence 5′-3′, forward | primer sequence 5′-3′, reverse | size (bp) |
|---|---|---|---|
| ALP | TGCAGTACGAGCTGAACAGG | TTTCTTGTCCGTGTCGCTCA | 341 |
| OC | CAACTGATCGACGGGCAGG | CTGGAGTTTATTGGGAGCAGC | 203 |
| COL I | CAATGGTGGCACCCAGTTTG | GGGCCAACGTCCACATAGAA | 390 |
| ON | GAACCACCACTGCAAACACG | TTGCCCTCATCCCTCTCGTA | 336 |
| OPN | AGACCCTCCCGAGTAAGTCC | GTGACTTTGGGTTTCCACGC | 506 |
| BMP-2 | GGAAGCTTTGGGAGACGACA | TGCACGATGGCATGGTTAGT | 564 |
| GAPDH | AGACACGATGGTGAAGGTCG | TGCCGTGGGTGGAATCATAC | 164 |

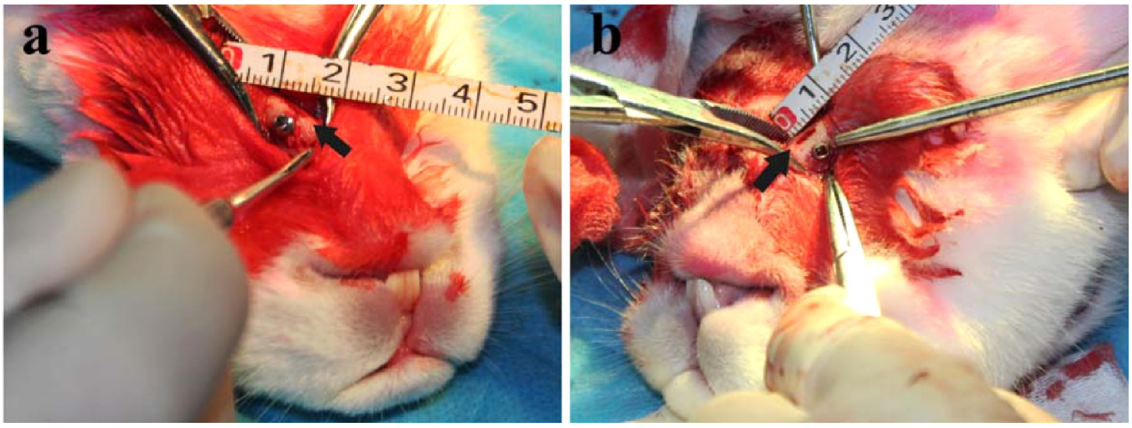


**Figure 1.** Images of implantation of 316L screw (a) and C-JDBM screw (b) in rabbit mandible bone. (Arrows: artificial defects).

deposited onto the matrix of the JDBM alloy. Calcium phosphate bioceramics have been proven to be biocompatible and osteoconductive with a more moderate degradation rate than that of magnesium alloy substitute for bone implants.[17−20] Niu et al.[21] had successfully deposited a calcium phosphate bioceramic coating (Ca−P coating, brushite, $CaHPO_4{\cdot}2H_2O$) onto JDBM samples with a bonding strength over 10 MPa and a thickness of 10−30 $\mu$m. In Niu's work, the Ca−P coating increased the corrosion resistance of JDBM samples in immersion and electrochemical tests. Hemolysis was significantly reduced and no obvious cytotoxicity was detected. However, the low compressive strength and fracture toughness remain instinctive drawbacks for their wider adhibition.[22] Therefore, the combination of the matrix of a Mg alloy with a Ca−P ceramic coating seems to be an effective solution for mandible bone implants. Hence, the JDBM alloy with specific surface treatment has shown potential as a next generation of degradable biomaterials. In this present work, we referenced Niu's work and conducted further evaluations for brushite-coated JDBM alloy used as mandibular bone repair. Reports of characteristics of biocompatibility, osteogenesis, and degradation of a JDBM alloy with a Ca−P coating for mandibular repair are presented.

## 2. MATERIALS AND METHODS

**2.1. Materials.** JDBM samples were prepared and brushite coating (approximately 10 MPa in bonding strength, 30 $\mu$m in thickness) were conducted as described before.[21] Samples of Φ19 × 3 mm were cut for extract preparation and Φ15 × 3 mm for direct cell adhesion assays.

**2.2. Preparation of Biomaterial Extracts.** According to ISO 10993,[2] one disk sample (Φ19 × 3 mm) was immersed in 6 mL of Dulbecco's modified Eagle's medium (DMEM, Gibco, Invitrogen) with 10% (w/v) fetal bovine serum (FBS, Gibco, Invitrogen), 100 units/mL penicillin (Gibco, Invitrogen), and 100 units/mL streptomycin (Gibco, Invitrogen). Extraction medium was incubated in a cell incubator (humidified atmosphere with 5% $CO_2$ at 37 °C) for 72 h. The supernatant was filtered and centrifuged afterward, refrigerated at 4 °C for use within 7 days.

**2.3. Isolation and Culture of Rabbit Bone Marrow Mesenchymal Stem Cells (rBM-MSCs).** Bone marrow was aspirated from iliac crest of anesthetized adult New Zealand white rabbits (weighted around 2.6 kg) and mixed with 1000 unit/mL preservative-free heparin. Approximately 5 mL of marrow was flushed with 5 mL of culture medium. Cells were plated at a density of $5 \times 10^6$ per Φ10 Petri dish after centrifugation and resuspension. Nonadherent cells were removed by changing culture medium after 5 days of incubation at 37 °C with 5% $CO_2$, humidified. Cells were detached and passaged after 14 days of primary culture with medium changed every 3 days when the monolayer cells reached 70% confluence. The purified third-passage cells were used for in vitro experiments.

**2.4. Cell Viability.** Bone marrow mesenchymal stem cells were seeded in a 96-well plate at a density of $5 \times 10^3$ cells per well and cultured with 100 $\mu$L extracts or culture medium as the negative control in each well for 1, 3, and 5 days, respectively. A Cell Counting Kit-8 (CCK-8, Beyotime, China) was performed following the manufacturer's protocol to assess cell viability. A total of 10 $\mu$L of CCK-8 dilution was added in each well, and the plates were incubated in a cell incubator for 1 h. Absorbance was read at 450 nm with a reference wavelength of 615 nm.

**2.5. In Vitro Cell Adhesion and Cell Morphology.** Disk samples (Φ15 × 3 mm) were immersed in culture medium for 10 min before 1 mL of $5 \times 10^4$/mL cell suspension was added onto each sample in a 24-well plate. After 24 h of incubation, the samples were stained with the vital dye calcein acetoxymethyl (Calcein-AM, Sigma, US) at a final concentration of 1 $\mu$g/mL for 30 min in a cell incubator. Observation was conducted by inverted fluorescence microscopy (IX 71, Olympus).

Prior to scanning electron microscopy (SEM) observation, samples were fixed in 2.5% glutaraldehyde (pH 7.4) at 4 °C for 2 h. Dehydration was carried out by 10 min of immersion in graded ethanol (50%, 70%, 80%, 90%, 95%, and 100%). Adherent cells were sputtered with gold, and cell morphology was observed by SEM analysis.

**2.6. Real-Time PCR.** Cells were seeded at a density of $1 \times 10^5$ cells per well in 6-well plates and cultured in osteogenic induction medium with 0.1 $\mu$M dexamethasone (Sigma), 50 $\mu$M ascorbate acid (Sigma), and 10 mM $\beta$-glycerophosphate (Sigma). The culture media were changed every 3 days.

Total RNA of rBM-MSCs was extracted with TRIzol reagent (Ambion, Life Technologies) following instructions after 12 and 18 days of culture in osteogenic differentiation medium. Total RNA quantification was performed by a NanoDrop spectrophotometer (NanoDrop Technologies). A total of 1 $\mu$g of RNA was pipetted into a 20 $\mu$L system using a reverse transcriptase kit (Toyobo, Japan). First strand cDNA synthesis was carried out in iScriptc DNA Synthesis (Bio-Rad). Standard 20 $\mu$L PCR reactions were prepared and programmed with 0.2 $\mu$L of cDNA as the template using SYBR green (Toyobo, Japan) detection in iCycler (Bio-Rad). The process included 1 min denaturation at 95 °C and 40 cycles (95 °C for 15 s, 60 °C for 15 s, 72 °C for 45 s) of PCR. Primer sequences of alkaline phosphatase (ALP), osteocalcin (OC), collagen I (COL I), osteonectin (ON), osteopotin (OPN), bone morphology protein-2 (BMP-2), and glyceraldehyde 3-phosphate dehydrogenase (GAPDH) are listed in Table 1. GAPDH was used as the housekeeping gene.

**2.7. Animal Model.** A total of 20 adult New Zealand rabbits of 2.6 ± 0.1 kg in weight were selected for the animal model in this work. Animals were anesthetized with an intramuscular injection of ketamine (0.5 mg/kg). Defects were artificially cut along the bottom of mandible bone in length of 2 mm. Randomly, 10 coated JDBM and 10 316L screws (2 mm in diameter and 4.6 mm in thread length) were implanted vertically into artificial defects in mandible bones (Figure 1). No damage of the brushite coating was made during the implantation. Samples were harvested 1, 4, and 7 months after surgery, respectively.

The experimental protocol was approved by the Animal Care and Experiment Committee of the School of Medicine, Fudan University.

**2.8. Serum Magnesium.** Blood samples were collected 1, 4, and 7 months postimplantation, respectively. Serum magnesium was determined after centrifugation by inductively coupled plasma mass spectrometry (ICP-MS, Agilent, US).

**2.9. Synchrotron Radiation X-ray Microtomography Analysis.** Synchrotron radiation X-ray microtomography (Shanghai Synchrotron Radiation Facility, China) was performed to evaluate the in vivo degradation of the implanted screws. Three-dimensional images were reconstructed based on the microtomography 2D slices using Amira (Visualization Science Group, US). In vivo degradation rates were calculated according to volume loss.

**2.10. Histological Evaluation.** Mandible bone tissues around screws were harvested 1, 4, and 7 months postimplantation and fixed in 10% neutral buffered formaldehyde for 2 weeks. After dehydration in a graded series of ethanol, undecalcified samples were embedded in poly(methyl methacrylate) (PMMA) and cut into 150 $\mu$m thick sections by a microtome (Leitz 1600, Microm, France). Then the sections were grinded and polished to a thickness of 50 ± 5 $\mu$m and stained with Van Gieson's picric acid-fuchsin.

Organs were collected and fixed in 10% formaldehyde solution and dehydrated before embedded in paraffin. Hematoxylin and eosin (HE) staining was performed on paraffin sections.

**2.11. SEM Observation and EDS Analysis.** Morphology of the PMMA sections was observed by scanning electron microscopy (SEM). Energy dispersive X-ray spectrum (EDS) analysis was applied to evaluate the degradation of brushite coating.

**2.12. Statistical Analysis.** All data are presented as the mean value ± standard deviation. Differences between groups were assessed by Student's *t*-test. A confidence level of 95% ($p < 0.05$) was considered statistically significant.

## 3. RESULTS

**3.1. Osmolality Adjustment and pH Value of Extracts.** Extracts of JDBM, brushite-coated JDBM (C-JDBM) and 316L stainless steel samples were prepared. According to previous studies,[23,24] standard extracts of biodegradable magnesium alloys were not suitable for in vitro evaluations. Overhigh osmolality and pH value would militate against cell viability, thus proper adjustment shall be made to the extracts in this work.

Figure 2 shows the osmolality and pH values of the three extracts and DMEM as negative control, using a freezing point

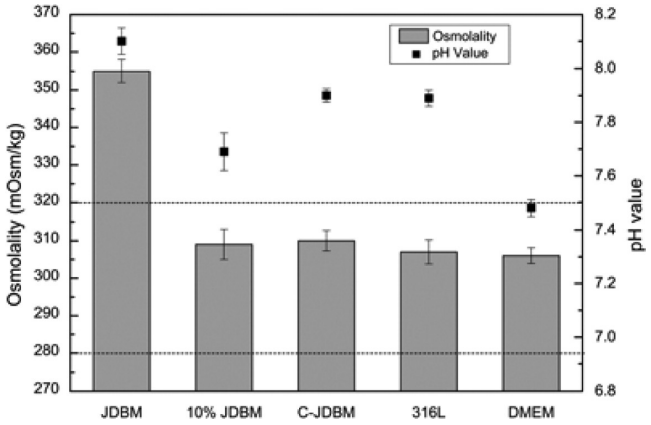


**Figure 2.** After 3 days of immersion, osmolality and pH value of extracts and culture medium. Osmolality of JDBM extract was normalized by a 10% dilution. (dashed line: reference level of osmolality).

osmometer (FM9X, SMUIF, China) and a pH meter (HANNA, Italy) respectively. After 3 days of degradation, excess $Mg^{2+}$ dissolved in the JDBM extract and led to an overstepped osmolality. Therefore, a 10% dilution (1 volume of extract and 9 volumes of DMEM) was applied to the JDBM extract for osmolality regulation.

**3.2. Cell Viability in Extracts.** Viability of rBM-MSCs cultured in 10% JDBM, C-JDBM, and 316L extracts is demonstrated in Figure 3. Cell viability was boosted on day 3

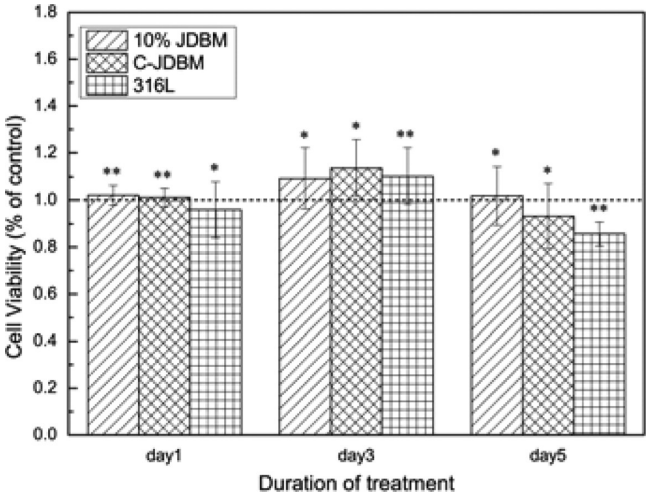


**Figure 3.** Viability of rBM-MSCs cultured in 10%-JDBM, C-JDBM, and 316L extracts for 1, 3, and 5 days. All three samples showed acceptable biocompatibility. (* $p < 0.05$, ** $p < 0.01$).

in all the experimental groups, especially in C-JDBM extract, which evidenced promotion of cell proliferation. Data of C-JDBM and 316L groups on day 5 indicate slightly adverse effects on cell viability.

**3.3. Cell Adhesion and Morphology.** The cell adhesion and morphology on JDBM, coated JDBM, and 316L samples of rBM-MSCs were evaluated in this work. Calcein-AM staining results and SEM morphology are shown in Figures 4 and 5. No obvious variance of cell density was observed in Figure 4, whereas diverse morphologies were evidenced, which is thought to be due to different surface roughness and surface chemistry.[25−27]

On all the surfaces, cells were well spread, elongated, and shaped as spindle, especially on JDBM samples. Cells were flatter

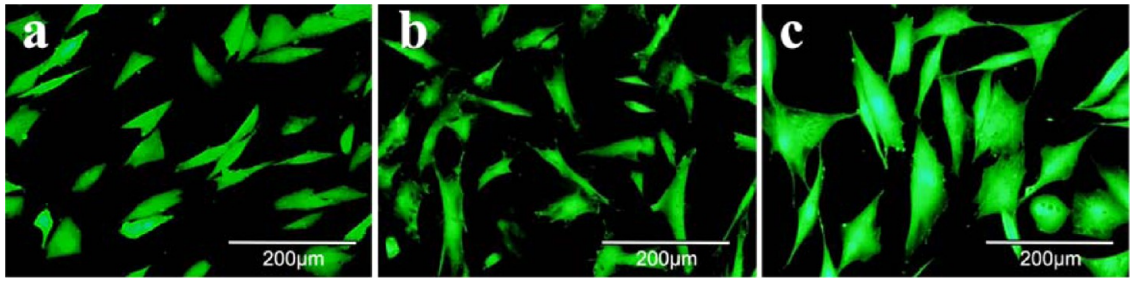


**Figure 4.** Calcein-AM stained rBM-MSCs adhered on surface of JDBM (a), C-JDBM (b), and 316L (c) samples after 24 h of culture.

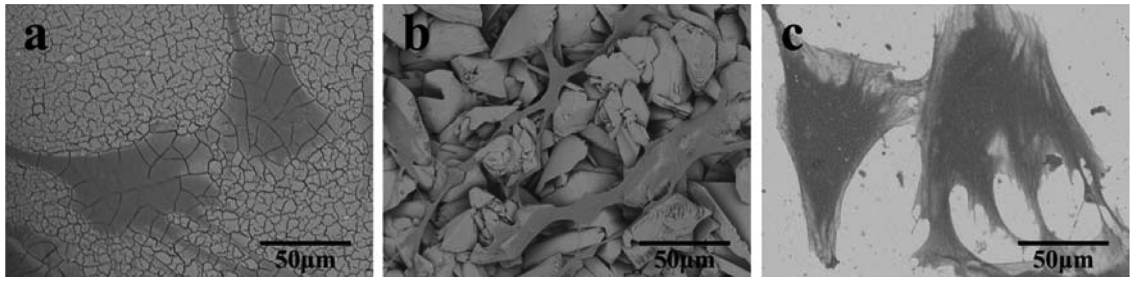


**Figure 5.** Morphologies of rBM-MSCs adhered on surface of JDBM (a), C-JDBM (b), and 316L (c) samples after 24 h of culture. Filopodia were tightly adhered on the substrates of the Ca−P coating (b).

on the surfaces of the JDBM and 316L samples than those on the coated JDBM sample. Filopodia were tightly adhered on the substrates of the Ca−P coating (Figure 5).

**3.4. Real-Time PCR.** RT-PCR results are shown in Figure 6. ALP expression of rBM-MSCs was highly improved by C-JDBM and 316L extracts on day 12. The JDBM extract did not show any positive influence on ALP expression until day 18. Both C-JDBM and 316L extracts induced type I collagen expression on day 12 and day 18, whereas type I collagen expression was only enhanced by JDBM extract on day 12. Expression of osteocalcin was significantly increased by 316L extract on day 18 and those of osteonectin and bone morphology protein-2 were highly raised by the C-JDBM extract on day 18. Only in the C-JDBM extract was osteopotin expression improved on day 12, whereas in other groups, it was not.

**3.5. Serum Magnesium.** Slight increase of serum magnesium of C-JDBM group was detected 1-month post implantation (Figure 7). Serum magnesium of C-JDBM group was higher than that of 316L group 1month post implantation. With prolonged implantation time, serum magnesium dropped gradually and reached the reference level in both 4 and 7 months.

**3.6. Synchrotron Radiation X-ray Microtomography Results.** The degradation of brushite-coated JDBM screws implanted in mandible bones of New Zealand White rabbits was studied using X-ray microtomography. Degraded screws could be visualized by three-dimensional reconstructions, as shown in Figure 8. An original model of the screw is demonstrated in Figure 8a. Degradation rates of brushite-coated JDBM after 1, 4, and 7 months of implantation were $0.161 \pm 0.075$, $0.097 \pm 0.013$, and $0.218 \pm 0.030$ mm/year, respectively. Basically, coated JDBM screws exhibited a favorable uniform corrosion mode, as shown in Figure 8b,c. A neck fracture was found on the JDBM screw (Figure 8d) after 7 month of implantation. Inference of residual stress while twisting screws was considered, which suggests a more optimized structure design of screws is necessary for further clinical applications.

**3.7. Histological Findings.** Bone regeneration after 1 and 4 months of implantation is shown in Figure 9. Foreign body reaction was weak and no inflammation process was observed for any samples.

In Figure 9, an asterisk represents artificial defects, and bone tissue was stained red. Osteoid (OI), osteoblasts (OB), and multinucleate cells (MC) were detected adjacent to the coated JDBM screws after 1 month postimplantation (Figure 9a,b). The bone trabecular was arranged in good order. Fibrous tissue and newly formed bone were clinging to the screw and growing along the thread, as shown in Figure 9a. Meanwhile, less immature bone tissue was observed and multinucleate cells were seldom seen around the 316L screw, as shown in Figure 9c,d. Osteocyte (OC) and osseous lamella were found in 4 months postoperation samples, indicating osteogenesis (Figure 9e,f). Mature bone tissue formed on the artificial defect site, as shown in Figure 9e.

To investigate whether any pathological change was caused by implantation, livers and kidneys were harvested after 7 months and stained on paraffin sections. Figure 10 shows HE staining of organ tissues of both groups. No tissue edema, inflammatory cells infiltrating, or fibrosis were found in liver cells arranged normally (Figure 10a,c). Proximal tubular epithelial cells (PTECs) were clear with no degeneration, congestion, or inflammatory cells (Figure 10b,d).

**3.8. SEM and EDS Analysis.** After 1 month of implantation, the majority of the brushite coating remained (30−40 $\mu$m in thickness) on the JDBM screws and the surface of the metal remained neat and smooth (Figure 11a). Immature bone tissue formed along the coating. Only an approximately 10 $\mu$m thick coating was found after 4 months of implantation. Thus, the surface of the JDBM screw was protected for the first 4 months of implantation until mature bone tissue formed. A 100 $\mu$m thick layer of corrosion products is seen in Figure 11c with an implantation time of 7 months, suggesting uniform degradation of the JDBM matrix.

## 4. DISCUSSION

**4.1. Biocompatibility of Brushite-Coated JDBM Alloy.** The objective of this study was to evaluate characteristics of the brushite-coated Mg−Nd−Zn−Zr alloy used for mandibular

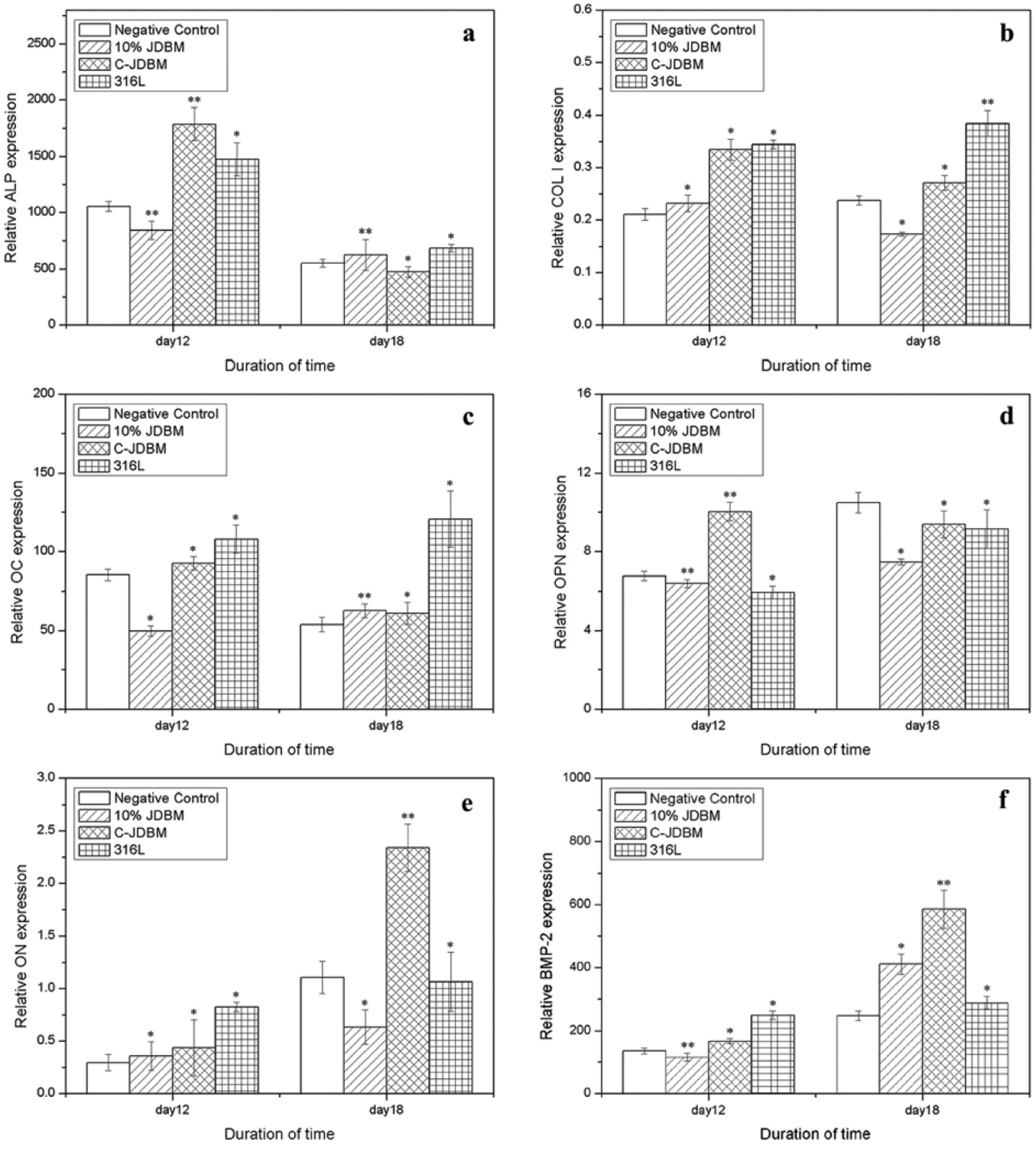


**Figure 6.** Results of RT-PCR for detection of expression of osteoblastic genes after 12 and 18 days of culture. (a) ALP, alkaline phosphatase; (b) COL I, type I collagen; (c) OC, osteocalcin; (d) OPN, osteopotin; (e) ON, osteonectin; (f) BMP-2, bone morphology protein-2. (* $p < 0.05$, ** $p < 0.01$).

repair. Both in vitro and in vivo experiments were carried out to build up a systematical evaluation of brushite-coated JDBM alloy and its potential for further applications.

Mg−Nd−Zn−Zr alloy has been proven to adopt a nanophasic biodegradation mechanism to enhance durability and biocompatibility;[15] a highly uniform array of nanopits with typical sizes less than 500 nm on the surface of a JDBM sample upon exposure to artificial plasma was observed. Although macroscopic pitting or delamination showed on the surface of the WE43 and AZ31 samples, which dominated the degradation process and resulted in a fast degradation rate and ultimately structural failure. With Ca−P coating, extract of the coated JDBM sample exhibited no evident increment in osmolality and pH value after 72 h of immersion, which indicated a well-protected surface of JDBM.

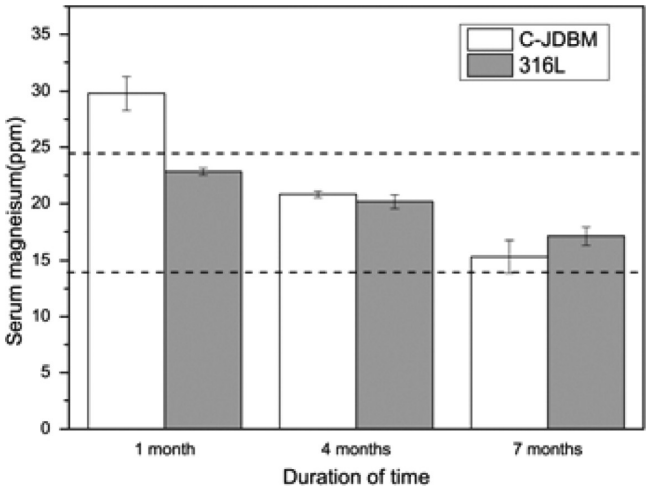


**Figure 7.** Serum magnesium of rabbits after 1, 4, and 7 months of implantation. (dashed line: range of serum magnesium level of healthy untreated New Zealand rabbits).

In vitro results evidenced biosafety, biocompatibility, and influence on osteoblastic differentiation of extracts of JDBM and C-JDBM with 316L stainless steel as the control. With a proper dilution and restoration of osmolality and pH value, rBM-MSCs responded positively in the presence of 10% JDBM extract. Due to the protection of the brushite coating, the C-JDBM samples released less $Mg^{2+}$ into its extract, which resulted in adequate osmolality and pH value for cell culture. Based in Figure 3, the C-JDBM extract promoted cell viability and proliferation of rBM-MSCs, especially on the third day of culture. According to ISO 10993-5,[28] brushite-coated JDBM meets the criteria of biosafety of surgical applications.

One of the crucial factors of bone substitute materials is the formation of an interface between substitute and bone tissue with mechanical stability.[18] A succession of processes comes along in the initial adhesion of cells with implants. Cell adhesion directly impacts cell growth, migration, and differentiation. Therefore, direct cellular adhesion and subsequent cellular responses are critical and prerequisite parameters for osteointegration and osteoconduction.[27,29−31] Calcein-AM staining and SEM observation in this study show that rBM-MSCs attached tightly on the surface of the JDBM, C-JDBM, and 316L samples. All three samples successfully facilitated cell attachment and spreading, which indicates adequate biocompatibility and potential osteogenesis of the Mg−Nd−Zn−Zr alloy and Ca−P coating.

Results of in vivo evaluations are consistent with in vitro experiments. No acute inflammation was detected for bone tissues around implanted screws. After 7 months of implantation, no pathological change of liver or kidney was found due to degradation of screws. Serum magnesium dropped to the normal level after a slight up-regulation in the first month of implantation on account of self-adjustment. Thus, brushite-coated JDBM alloy used as mandibular bone repair material is proven to be biocompatible from present work.

**4.2. Osteogenic Differentiation of rBM-MSCs.** Influence of osteogenic differentiation of rBM-MSCs by extracts of JDBM, C-JDBM and 316L is evaluated by RT-PCR, as shown in Figure 6. Differentiation of rBM-MSCs is one of the key processes for bone regeneration. ALP is the most widely recognized marker of osteoblastic differentiation.[32] It is a cell surface glycoprotein and is involved in mineralization.[33]As an early differentiation marker,[34] up regulation of ALP expression occurred on 12th day in C-JDBM and 316L extracts (Figure 6 (a)), meaning the promotion of mineralization of rBM-MSCs by C-JDBM and 316L extracts. OC, one of the major osteoblastic differentiation products, is synthesized only by mature osteoblasts, osontoblasts and cementoblasts. OPN, produced by osteoblasts, is a prominent component of mineralized extracellular matrix of bone. The up-regulation of OPN expression associates with bone mineralization and formation.[35] BMP-2 participates in the osteoblast differentiation, as well as in the enhancement of bone matrix production.[36,37] Type I collagen is one of the most copious proteins in extracellular bone matrix. ON is in operation of binding to both collagen and calcium.[38,39] Therefore, expressions of these genes are indicators of osteoblastic differentiation. Expressions of COL I, OC, OPN, ON and BMP-2 (Figure 6 (b-f)) were all up regulated in C-JDBM extract after 12 and 18 days of culture. Brushite-coated JDBM samples showed better osteoblastic differentiation inductivity than uncoated JDBM and 316L samples, which indicates that brushite coating is an effective way to enhance osteoblastic differentiation of rBM-MSCs.

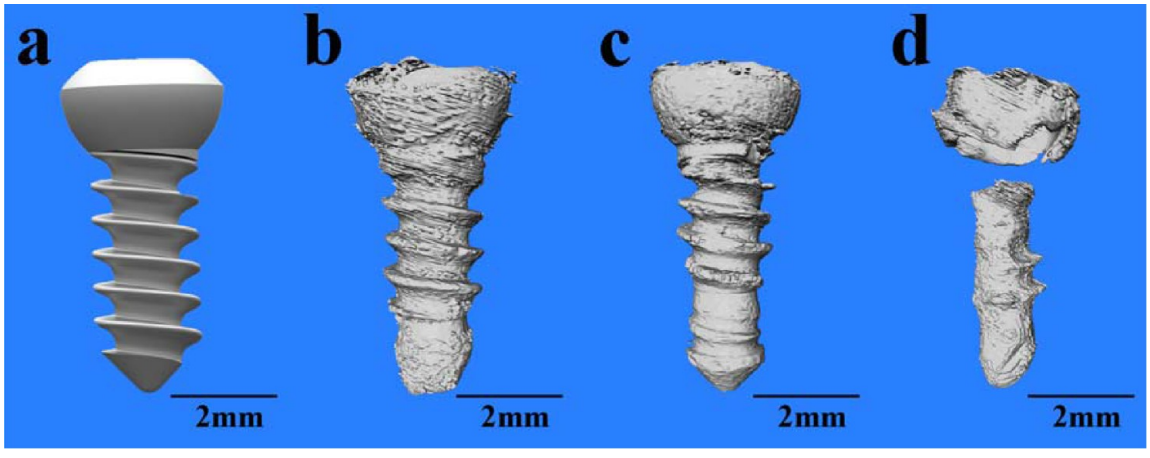


**Figure 8.** Picture of original screw model (a) and 3D reconstruction images of C-JDBM screws after 1 (b), 4 (c), and 7 (d) months of implantation. No obvious degradation happened 1 month (b) postimplantation. Slight volume loss was found 4 months (c) postimplantation. Magnesium screw seriously degraded after 7 months (d) of implantation.

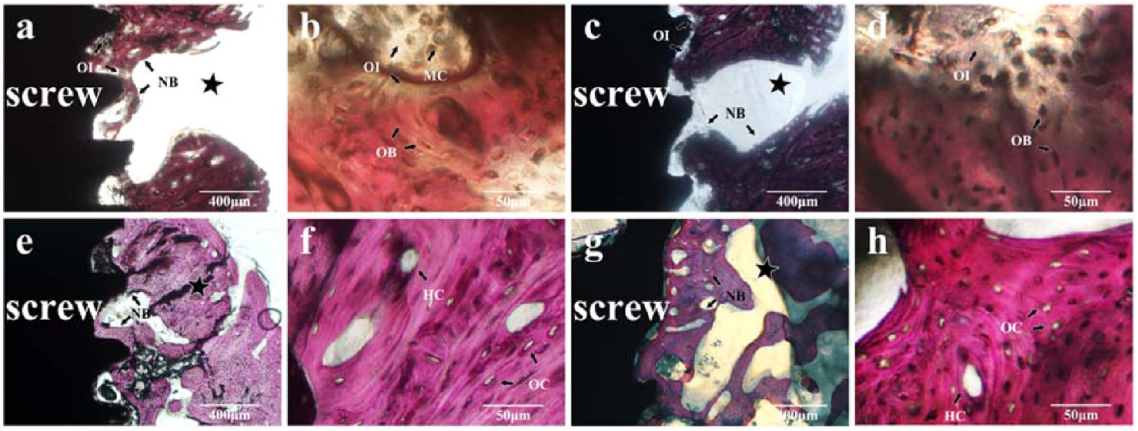


**Figure 9.** Histological morphologies of implanted C-JDBM (a, b, e, f) and 316L (c, d, g, h) screws and bone tissue after 1 (a-d) and 4 (e-h) months of implantation. NB: new bone, OI: osteoid, MC: multinucleate cell, OB: osteoblast, HC: haversian canal, OC: osteocyte, asterisk: artificial defect.

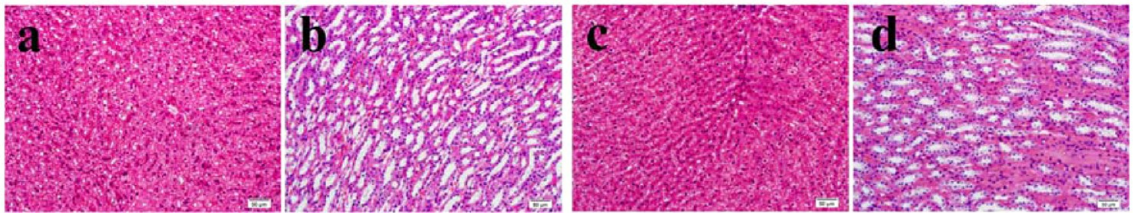


**Figure 10.** Results of HE staining of liver (a, c) and kidney (b, d) tissue of C-JDBM (a, b), and 316L (c, d) groups after 7 months of implantation.

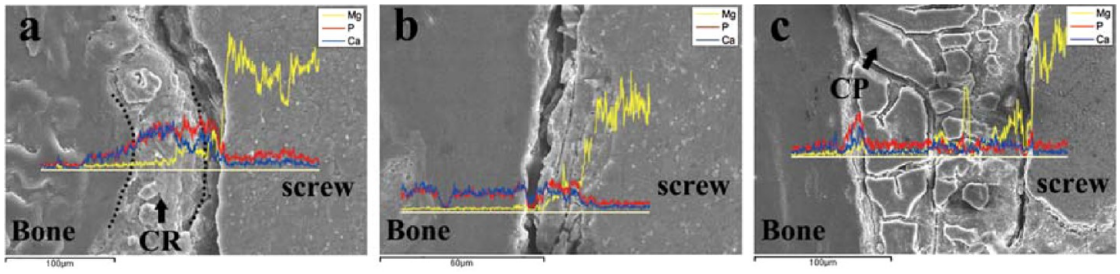


**Figure 11.** SEM micrographs and EDS analysis of C-JDBM screws after 1 (a), 4 (b), and 7 (c) months of implantation. CR, coating residue; CP, corrosion product.

**4.3. Osteogenesis and Degradation Control by Brushite Coating.** Ca−P biomaterials have been proven to have many desirable properties.[18,40] Similar composition to bone mineral endows Ca−P bioceramic with a particular strong interface with bone, which leads to bioactivity and osteoconductivity. Histology findings revealed osteogenesis and osteoconductivity of brushite coating of JDBM screws as mandibular repair material. Much more osteoid (46% in area, Figure 9 (b)) and immature bone tissues formed with an intimate interface with brushite-coated JDBM screw while less osteoid (29% in area, Figure 9 (d)) was found around 316L screw with a gap between bone tissue and screw as shown in Figure 9 (a-d). Mature bone formed around brushite-coated JDBM screw after 4 months of implantation and bone tissue had covered artificial defect (Figure 9 (e, f)). However, less area of bone tissue (58% in Figure 9 (g), 87% in Figure 9 (e)) was observed around 316L screws. Histology findings showed that Ca−P-coated JDBM alloy is superior to 316L stainless steel in performance of osteogenesis and osteoconductivity as a mandibular bone repair material.

Other than osteogenesis and osteoconductivity, Ca−P bioceramic coating also enhanced biocorrosion resistance of degradable JDBM alloy. Forming a protective layer of bone-like apatite or carbonate hydroxyapatite[41,42] on its surface reduces in vivo degradation rate of the Mg alloy. In vivo evaluation showed effective biocorrosion resistance in the early stage of implantation. Ca−P coating protected metal screws from degrading during the formation of immature bone tissue around the coating. Degradation rate was only 0.161 ± 0.025 mm/year in the first month of implantation. Along with the formation of apatite layer and duration of time, degradation rate decreased to 0.097 ± 0.013 mm/year within 4 months of implantation. By the time when mature bone tissue formed and artificial defect was healed, Ca−P coating was almost dissolved and metal matrix began to degrade. Meanwhile, degradation rate had reached to 0.218 ± 0.030 mm/year within 7 months of implantation. According to this rate, a brushite-coated JDBM screw would completely degrade after 10 to 12 months of implantation. Specific evaluations of completed degradation time will be carried out in future works. Therefore, under the synergetic effect of the brushite coating and the slow uniform degradation of JDBM matrix, the brushite-coated JDBM bone implants exhibited clinical acceptable degradation behavior by which the

risk for fracture failure of the implants by redundant loadings in mandible bone will be eliminated to a certain degree.

## 5. CONCLUSIONS

Both JDBM and brushite-coated JDBM samples showed adequate biosafety and biocompatibility as bone repair substitute for in vitro evaluations. Rabbit bone marrow mesenchymal stem cells responded positively not only in the extract of C-JDBM but also on the surface of C-JDBM samples, which is prerequisite for a bone repair material. According to the results of RT-PCR, extract of brushite-coated JDBM considerably induced expressions of different markers of osteogenic differentiation to various degrees. The promotion of osteogenic differentiation of brushite-coated JDBM reveals clues of osteogeneration acceleration in vivo as mandibular bone repair material. In vivo evaluations confirmed results of in vitro experiments and evidenced advantage, comparing to 316L screws, in osteoconductivity and osteogenesis of brushite-coated JDBM screws implanted in rabbit mandible bones. Furthermore, due to its lower biodegradation rate and a protective layer of bone-like apatite formed after implantation, brushite coating significantly reduced degradation rate of biodegradable JDBM screws at the initial stage of implantation, comparing to that of 7-month postoperation without protection of the coating. With accomplishment of new bone formation, JDBM screw kept degrading at an acceptable rate with an estimated degradation time of 10 to 12 months in total, which is in need of confirmation in future works. Therefore, not only bone regeneration was enhanced but also an effective degradation control was brought out by a combination of bioactive brushite coating and uniform biodegradable JDBM matrix, indicating that the Mg−Nd−Zn-Zr alloy with brushite coating possesses great potential for applications as a mandibular repair material.

## AUTHOR INFORMATION


### Corresponding Author

*G. Yuan. E-mail: gyyuan@sjtu.edu.cn.

### Author Contributions

⊥These authors contributed equally to this work (X. G. and M. X.).


### Notes

The authors declare no competing financial interest.

## ACKNOWLEDGMENTS

The authors gratefully acknowledge the support by Major Basic Research Project of Shanghai, Science and Technology Commission (Grant No. 11DJ1400301), Natural Science Funds of Minhang District, Shanghai City (Grant No. 2011MHZ23), and Special Research Foundation of Young Teachers of Shanghai Medical, College of Fudan University (Grant No. 11L-36).

## REFERENCES


(1) Walker, J.; Shadanbaz, S.; Woodfield, T. B.; Staiger, M. P.; Dias, G. J. Magnesium Biomaterials for Orthopedic Application: A Review from a Biological Perspective. *J. Biomed. Mater. Res., Part B* **2014**, *102*, 1316−1331.

(2) Witte, F.; Kaese, V.; Haferkamp, H.; Switzer, E.; Meyer-Lindenberg, A.; Wirth, C.; Windhagen, H. In Vivo Corrosion of Four Magnesium Alloys and the Associated Bone Response. *Biomaterials* **2005**, *26*, 3557−3563.

(3) Habibovic, P.; Barralet, J. E. Bioinorganics and Biomaterials: Bone Repair. *Acta Biomater.* **2011**, *7*, 3013−26.

(4) Li, N.; Zheng, Y. Novel Magnesium Alloys Developed for Biomedical Application: A Review. *J. Mater. Sci. Technol.* **2013**, *29*, 489−502.

(5) Witte, F.; Fischer, J.; Nellesen, J.; Crostack, H. A.; Kaese, V.; Pisch, A.; Beckmann, F.; Windhagen, H. In Vitro and in Vivo Corrosion Measurements of Magnesium Alloys. *Biomaterials* **2006**, *27*, 1013−8.

(6) Zhang, E.; Xu, L.; Yu, G.; Pan, F.; Yang, K. In Vivo Evaluation of Biodegradable Magnesium Alloy Bone Implant in the First 6 Months Implantation. *J. Biomed. Mater. Res., Part A* **2009**, *90*, 882−893.

(7) Janning, C.; Willbold, E.; Vogt, C.; Nellesen, J.; Meyer-Lindenberg, A.; Windhagen, H.; Thorey, F.; Witte, F. Magnesium Hydroxide Temporarily Enhancing Osteoblast Activity and Decreasing the Osteoclast Number in Peri-Implant Bone Remodelling. *Acta Biomater.* **2010**, *6*, 1861−1868.

(8) Hampp, C.; Ullmann, B.; Reifenrath, J.; Angrisani, N.; Dziuba, D.; Bormann, D.; Seitz, J. M. Meyer-Lindenberg, A. Research on the Biocompatibility of the New Magnesium Alloy Land442—An in Vivo Study in the Rabbit Tibia over 26 Weeks. *Adv. Eng. Mater.* **2012**, *14*, B28−B37.

(9) Erdmann, N.; Angrisani, N.; Reifenrath, J.; Lucas, A.; Thorey, F.; Bormann, D.; Meyer-Lindenberg, A. Biomechanical Testing and Degradation Analysis of Mgca0. 8 Alloy Screws: A Comparative in Vivo Study in Rabbits. *Acta Biomater.* **2011**, *7*, 1421−1428.

(10) Willbold, E.; Kaya, A.; Kaya, R.; Beckmann, F.; Witte, F. Corrosion of Magnesium Alloy Az31 Screws Is Dependent on the Implantation Site. *Mater. Sci. Eng.* **2011**, *176*, 1835−1840.

(11) Van Den Bos, T.; Speijer, D.; Bank, R. A.; Bromme, D.; Everts, V. Differences in Matrix Composition between Calvaria and Long Bone in Mice Suggest Differences in Biomechanical Properties and Resorption: Special Emphasis on Collagen. *Bone* **2008**, *43*, 459−68.

(12) Yuan, G.; Zhang, X.; Ding, W. In Vivo Biodegradable Magnesium Alloy Implant Material with High Strength and Ductility as Well as Excellent Biocorrosion Resistance. Chinese Patent No. ZL2010102047, September 19, 2010.

(13) Song, G. Control of Biodegradation of Biocompatable Magnesium Alloys. *Corros. Sci.* **2007**, *49*, 1696−1701.

(14) Zhang, X.; Yuan, G.; Mao, L.; Niu, J.; Fu, P.; Ding, W. Effects of Extrusion and Heat Treatment on the Mechanical Properties and Biocorrosion Behaviors of a Mg-Nd-Zn-Zr Alloy. *J. Mech. Behav. Biomed. Mater.* **2012**, *7*, 77−86.

(15) Mao, L.; Shen, L.; Niu, J.; Zhang, J.; Ding, W.; Wu, Y.; Fan, R.; Yuan, G. Nanophasic Biodegradation Enhances the Durability and Biocompatibility of Magnesium Alloys for the Next-Generation Vascular Stents. *Nanoscale* **2013**, *5*, 9517−9522.

(16) Yang, C.; Yuan, G.; Zhang, J.; Tang, Z.; Zhang, X.; Dai, K. Effects of Magnesium Alloys Extracts on Adult Human Bone Marrow-Derived Stromal Cell Viability and Osteogenic Differentiation. *Biomed. Mater.* **2010**, *5*, 045005.

(17) Xin, R.; Leng, Y.; Chen, J.; Zhang, Q. A Comparative Study of Calcium Phosphate Formation on Bioceramics in Vitro and in Vivo. *Biomaterials* **2005**, *26*, 6477−6486.

(18) LeGeros, R. Z. Properties of Osteoconductive Biomaterials: Calcium Phosphates. *Clin. Orthop. Relat. Res.* **2002**, *395*, 81−98.

(19) Thein-Han, W.; Liu, J.; Xu, H. H. K. Calcium Phosphate Cement with Biofunctional Agents and Stem Cell Seeding for Dental and Craniofacial Bone Repair. *Dent. Mater.* **2012**, *28*, 1059−1070.

(20) LeGeros, R. Z. Calcium Phosphate-based Osteoinductive Materials. *Chem. Rev.* **2008**, *108*, 4742−4753.

(21) Niu, J.; Yuan, G.; Liao, Y.; Mao, L.; Zhang, J.; Wang, Y.; Huang, F.; Jiang, Y.; He, Y.; Ding, W. Enhanced Biocorrosion Resistance and Biocompatibility of Degradable Mg-Nd-Zn-Zr Alloy by Brushite Coating. *Mater. Sci. Eng., C* **2013**, *33*, 4833−41.

(22) Mehdawi, I. M.; Pratten, J.; Spratt, D. A.; Knowles, J. C.; Young, A. M. High Strength Re-Mineralizing, Antibacterial Dental Composites with Reactive Calcium Phosphates. *Dent. Mater.* **2013**, *29*, 473−484.

(23) Fischer, J.; Prosenc, M. H.; Wolff, M.; Hort, N.; Willumeit, R.; Feyerabend, F. Interference of Magnesium Corrosion with Tetrazolium-based Cytotoxicity Assays. *Acta Biomater.* **2010**, *6*, 1813−1823.

(24) Hänzi, A. C.; Gerber, I.; Schinhammer, M.; Löffler, J. F.; Uggowitzer, P. J. On the in Vitro and in Vivo Degradation Performance and Biological Response of New Biodegradable Mg−Y−Zn Alloys. *Acta Biomater.* **2010**, *6*, 1824−1833.
(25) Divya Rani, V. V.; Vinoth-Kumar, L.; Anitha, V. C.; Manzoor, K.; Deepthy, M.; Shantikumar, V. N. Osteointegration of Titanium Implant Is Sensitive to Specific Nanostructure Morphology. *Acta Biomater.* **2012**, *8*, 1976−1989.
(26) Liu, P.; Domingue, E.; Ayers, D. C.; Song, J. Modification of Ti6Al4V Substrates with Well-Defined Zwitterionic Polysulfobetaine Brushes for Improved Surface Mineralization. *ACS Appl. Mater. Interfaces* **2014**, *6*, 7141−52.
(27) Liang, C.; Wang, H.; Yang, J.; Cai, Y.; Hu, X.; Yang, Y.; Li, B.; Li, H.; Li, H.; Li, C.; Yang, X. Femtosecond Laser-Induced Micropattern and Ca/P Deposition on Ti Implant Surface and Its Acceleration on Early Osseointegration. *ACS Appl. Mater. Interfaces* **2013**, *5*, 8179−86.
(28) International Organization for Standardization. *ISO B 10993-5: Biological Evaluation of Medical Devices−Part 5: Tests for in Vitro Cytotoxicity*; ISO: Geneva, Switzerland, 1999.
(29) Burridge, K.; Fath, K.; Kelly, T.; Nuckolls, G.; Turner, C. Focal Adhesions: Transmembrane Junctions between the Extracellular Matrix and the Cytoskeleton. *Annu. Rev. Cell Biol.* **1988**, *4*, 487−525.
(30) Anselme, K. Osteoblast Adhesion on Biomaterials. *Biomaterials* **2000**, *21*, 667−681.
(31) Kieswetter, K.; Schwartz, Z.; Dean, D.; Boyan, B. The Role of Implant Surface Characteristics in the Healing of Bone. *Crit. Rev. Oral Biol. Med.* **1996**, *7*, 329−345.
(32) Stucki, U.; Schmid, J.; Hämmerle, C.; Lang, N. Temporal and Local Appearance of Alkaline Phosphatase Activity in Early Stages of Guided Bone Regeneration. *Clin. Oral Implants Res.* **2001**, *12*, 121−127.
(33) Marom, R.; Shur, I.; Solomon, R.; Benayahu, D. Characterization of Adhesion and Differentiation Markers of Osteogenic Marrow Stromal Cells. *J. Cell. Physiol.* **2005**, *202*, 41−48.
(34) Dalby, M. J.; Gadegaard, N.; Tare, R.; Andar, A.; Riehle, M. O.; Herzyk, P.; Wilkinson, C. D.; Oreffo, R. O. The Control of Human Mesenchymal Cell Differentiation Using Nanoscale Symmetry and Disorder. *Nat. Mater.* **2007**, *6*, 997−1003.
(35) Franceschi, R. The Developmental Control of Osteoblast-Specific Gene Expression: Role of Specific Transcription Factors and the Extracellular Matrix Environment. *Crit. Rev. Oral Biol. Med.* **1999**, *10*, 40−57.
(36) Susperregui, A. R.; Viñals, F.; Ho, P. W.; Gillespie, M. T.; Martin, T. J.; Ventura, F. BMP-2 Regulation of PTHrP and Osteoclastogenic Factors During Osteoblast Differentiation of C2c12 Cells. *J. Cell. Physiol.* **2008**, *216*, 144−152.
(37) Liu, X.; Zhao, K.; Gong, T.; Song, J.; Bao, C.; Luo, E.; Weng, J.; Zhou, S. Delivery of Growth Factors Using a Smart Porous Nanocomposite Scaffold to Repair a Mandibular Bone Defect. *Biomacromolecules* **2014**, *15*, 1019−30.
(38) Bolander, M. E.; Young, M. F.; Fisher, L. W.; Yamada, Y.; Termine, J. D. Osteonectin Cdna Sequence Reveals Potential Binding Regions for Calcium and Hydroxyapatite and Shows Homologies with Both a Basement Membrane Protein (Sparc) and a Serine Proteinase Inhibitor (Ovomucoid). *Proc. Natl. Acad. Sci. U. S. A.* **1988**, *85*, 2919−2923.
(39) Romberg, R.; Werness, P.; Lollar, P.; Riggs, B. L.; Mann, K. Isolation and Characterization of Native Adult Osteonectin. *J. Biol. Chem.* **1985**, *260*, 2728−2736.
(40) Mohedano, M.; Matykina, E.; Arrabal, R.; Pardo, A.; Merino, M. C. Metal Release from Ceramic Coatings for Dental Implants. *Dent. Mater.* **2014**, *30*, e28−40.
(41) Boyde, A.; Corsi, A.; Quarto, R.; Cancedda, R.; Bianco, P. Osteoconduction in Large Macroporous Hydroxyapatite Ceramic Implants: Evidence for a Complementary Integration and Disintegration Mechanism. *Bone* **1999**, *24*, 579−589.
(42) Zhang, X.; Li, X. W.; Li, J. G.; Sun, X. D. Preparation and Characterizations of Bioglass Ceramic Cement/Ca-P Coating on Pure Magnesium for Biomedical Applications. *ACS Appl. Mater. Interfaces* **2014**, *6*, 513−25.